nature chemistry

ARTICLES

PUBLISHED ONLINE: XX XX 2017 | DOI: 10.1038/NCHEM.2818

Single-molecule spectroscopy of LHCSR1 protein dynamics identifies two distinct states responsible for multi-timescale photosynthetic photoprotection

Toru Kondo[1], Alberta Pinnola[2], Wei Jia Chen[1], Luca Dall'Osto[2], Roberto Bassi[2,3]
Q1 and Gabriela S. Schlau-Cohen[1]*

In oxygenic photosynthesis, light harvesting is regulated to safely dissipate excess energy and prevent the formation of harmful photoproducts. Regulation is known to be necessary for fitness, but the molecular mechanisms are not understood. One challenge has been that ensemble experiments average over active and dissipative behaviours, preventing identification of distinct states. Here, we use single-molecule spectroscopy to uncover the photoprotective states and dynamics of the light-harvesting complex stress-related 1 (LHCSR1) protein, which is responsible for dissipation in green algae and moss. We discover the existence of two dissipative states. We find that one of these states is activated by pH and the other by carotenoid composition, and that distinct protein dynamics regulate these states. Together, these two states enable the organism to respond to two types of intermittency in solar intensity—step changes (clouds and shadows) and ramp changes (sunrise), respectively. Our findings reveal key control mechanisms underlying photoprotective dissipation, with implications for increasing biomass yields and developing robust solar energy devices.

Photosynthetic light-harvesting complexes (LHCs) capture solar energy and feed it to downstream molecular machinery[1]. When light absorption exceeds the capacity for utilization, the excess energy can generate singlet oxygen, which causes cellular damage. Thus, in oxygenic photosynthesis, LHCs have evolved a feedback loop that triggers photoprotective energy dissipation[2–4]. The crucial importance of photoprotection for fitness has been demonstrated, as well as its impact on biomass yields[5]. Recent efforts to rewire photoprotection have demonstrated an impressive 20% increase in biomass[6]. However, the mechanisms of photoprotection—from the fast photophysics of the pigments to the slow conformational changes of proteins—have not yet been resolved. The lack of mechanistic understanding is a major limitation in the speed and efficacy of improving biomass yields.

Collectively, the photoprotective mechanisms are known as non-photochemical quenching (NPQ). NPQ involves changes to the photophysics, conformation and organization of LHCs within the membrane[2–4]. The seconds to minutes component of NPQ is the dissipation of excess sunlight within the LHCs. The LHCs consist of pigments (chlorophyll and carotenoids) closely packed within a protein matrix. The carotenoid composition is controlled by light conditions via the xanthophyll cycle, in which violaxanthin (Vio) is converted to zeaxanthin (Zea) under high light conditions. Most LHCs are primarily responsible for light harvesting, but in recent research, one of the LHCs, light-harvesting complex stress-related (LHCSR) protein, was identified as the key gene product for the dissipation of excess sunlight in unicellular algae and mosses[7–14]. LHCSR consists of chlorophyll-*a* and carotenoids held within a protein matrix[8,12,15]. Activation of dissipation in LHCSR occurs based on three functional parameters: (1) low pH[8,16–18], (2) binding of zeaxanthin[11] and (3) interactions with surrounding proteins[10,13]. Although the carotenoid has been implicated in dissipation, several mechanisms have been proposed: energy transfer to the carotenoid[19,20]; a state with mixed chlorophyll/carotenoid character[21]; and the formation of a charge-transfer state between the chlorophyll and the carotenoid[22–24]. Recent results suggest that quenching may rely on more than one of these mechanisms[25].

Despite these extensive studies, the dissipative states and their individual conformational and photophysical dynamics have not been identified. One major barrier to identifying individual conformations is that the difference between states is often small and the transitions between them occur asynchronously. Thus, ensemble experiments average over these states and their dynamics. To overcome this limitation, we performed the first single-molecule fluorescence measurements on LHCSR1, one of the LHCSR proteins[11,18]. Quenching of the fluorescence emission, often accompanied by changes in the fluorescence lifetime and spectrum, reports on non-radiative decay or dissipation as studied in plant LHCs[26–30]. With this reporter, we explored the dissipative and non-dissipative states. We identified these states and their likely conformational and photophysical origins, gaining molecular-level insight into photoprotection.

We characterized the intrinsic dynamics between the different photophysical states of LHCSR1 that are generally regarded to represent different conformational and photoprotective states. These are the dynamics exhibited under experimental conditions that mimic low to medium light. These intrinsic dynamics, which occur more rapidly than those in plant LHCs[26,27,29], reveal that the presence of LHCSR1, independent of regulatory parameters, is able to play a photoprotective role. Indeed, expression levels of

[1]Department of Chemistry, Massachusetts Institute of Technology, 77 Massachusetts Avenue, Cambridge, Massachusetts 02139, USA. [2]Department of Biotechnology, University of Verona, Cà Vignil 1, Strada Le Grazie 15, 37134, Verona, Italy. [3]Istituto per la Protezione delle Piante (IPP), Consiglio Nazionale delle Ricerche (CNR), Strada delle Cacce 73, 10135, Turin, Italy. *e-mail: gssc@mit.edu Q2

LHCSR1 increase with light intensity in most species, in agreement with this result[7,9]. We also uncovered the regulated conformational dynamics, which are the dynamics that change through a cellular feedback loop responsive to solar intensity. Notably, within the regulated conformational dynamics, we found two dissipative states, where the population of one of these states is primarily controlled by pH and the other by carotenoid composition, revealing the distinct roles of these two functional parameters. With this approach we also compared LHCSR1 to a light-harvesting complex (LHCB1) protein. The results from this comparison suggest that photoprotective functionality may have evolved by harnessing and optimizing the conformational heterogeneity of the protein structure, which has also been observed in plant LHCs[26,29]. The conformational and photophysical dynamics of LHCSR1 enable multiple quenching mechanisms, and thus multiple response times, to regulate the multi-timescale changes in solar intensity. The ability to leverage the photophysics of the embedded chlorophyll to clearly observe conformational dynamics within LHCSR1 enables a mechanistic exploration of biological regulation.

Results

Fluorescence intensity and lifetime of single LHCSR1 and LHCB1. Figure 1 presents representative time traces of fluorescence intensity and lifetime for single LHCSR1s and LHCB1s incorporating Vio and Zea at pH 7.5 and pH 5. The pH levels reproduce lumenal pH under low and high light, Q3 respectively. As shown in Fig. 1a, for single LHCSR1s containing Vio at pH 7.5 (LHCSR1-V-7.5), the intensity and lifetime synchronously change from low to high levels (periods 1 and 2, respectively), fluctuate (period 3), and finally fall to the dark level (the particle is photobleached).

For LHCSR1-V-7.5 (period 3, Fig. 1a) and LHCSR1-Z-7.5 (period 4, Fig. 1c) there are frequent rapid fluctuations between the low and high emissive levels, although the lifetimes are shorter overall when Zea is incorporated (Supplementary Fig. 2). A decrease in pH to 5 (LHCSR1-V-5 and LHCSR1-Z-5) suppresses these fluctuations. Instead, stable emission at low intensity and short lifetime is observed (Fig. 1b,d).

For LHCB1, no rapid and large fluctuations of fluorescence intensity and lifetime between emissive levels are observed (Fig. 1e). Additionally, LHCB1 at pH 7.5 (LHCB1-7.5) exhibits a larger variety of combinations of fluorescence intensity and lifetime. However, the intensity and lifetime levels decrease in LHCB1 at low pH (LHCB1-5) (Fig. 1f), similarly to LHCSR1 (Fig. 1b,d).

Intensity–lifetime probability distribution. To identify the states defined by the fluorescent properties, we determined the normalized two-dimensional histograms for fluorescence intensity and lifetime of LHCSR1 and LHCB1 (Fig. 2a–f). In these histograms, clusters emerge that represent different states, very probably corresponding to different conformations.

LHCSR1-V-7.5 shows two states with high intensity and long lifetime (state I) and low intensity and short lifetime (state III) (Fig. 2a). Thus, state I is unquenched and state III is quenched (dissipative). In the presence of Zea (Fig. 2c), the relative population of state III increases and state I is displaced by state II, which exhibits an intermediate intensity and lifetime and so is partially quenched.

At low pH, state II′ appears with low intensity and an intermediate lifetime (Fig. 2b,d). In the presence of Vio, the probability of state II′ is dominant (Fig. 2b). However, the conversion of Vio to Zea increases the probability of state III (Fig. 2d), similar to the behaviour at pH 7.5.

In contrast to the distinct states in LHCSR1, in LHCB1-7.5 the probability distribution covers a wide area in fluorescence intensity and lifetime (Fig. 2e). States I′ and I, with long lifetimes and low and high intensities, respectively, decrease in relative population at pH 5

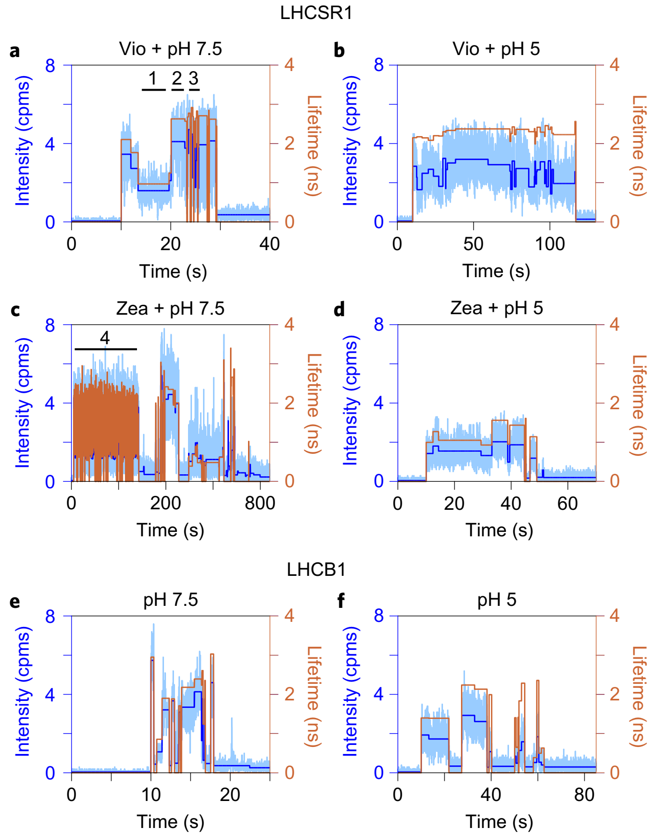

Figure 1 | Time traces of fluorescence intensity and lifetime of LHCSR1 and LHCB1. a–f, Time traces of single LHCSR1 with Vio at pH 7.5 (**a**) and pH 5 (**b**), Zea-enriched LHCSR1 at pH 7.5 (**c**) and pH 5 (**d**) and LHCB1 at pH 7.5 (**e**) and pH 5 (**f**). The number of photons is binned at 10 ms (light blue, left axis) and displayed along with the intensity levels determined through a change-point-finding algorithm (blue, left axis). The lifetime (orange, right axis) was estimated by histograming all photons for each intensity level. Excitation light was turned on at 10 s. The time regions labelled 1–4 indicate representative behaviours for each condition. Other examples are provided in Supplementary Fig. 2.

(Fig. 2f). States II′ and II, with intermediate lifetimes, appear, and state III increases in relative population. Overall, the pH drop slightly quenches the fluorescence in LHCB1, to a far lower extent than in LHCSR1 (Fig. 2b,d).

Conformational transitions in single LHCSR1 and LHCB1. Protein dynamics between the states were investigated by exploring the transitions between the levels of constant intensity (for example, from period 1 to period 2 in Fig. 1a). Two-dimensional histograms of these transitions were constructed and normalized (Fig. 2g–l). For LHCSR1-V-7.5 (Fig. 2g), area i indicates positive shifts of intensity and lifetime, with $\Delta I \approx 2$ cpms Q4 and $\Delta\tau \approx 2$ ns, corresponding to the transition from state III to I in Fig. 2a. Area ii indicates the reverse transition from state I to III. The high probabilities in areas i and ii correspond to the frequent fluctuations observed in the time traces of fluorescence in LHCSR1-V-7.5 (period 3 in Fig. 1a and period 5 in Supplementary Fig. 2). The small shifts of intensity and lifetime (period 6 in Supplementary Fig. 2), corresponding to the protein dynamics within a state, appear in area iii. In LHCSR1-Z-7.5, the same features are observed (Fig. 2i), although the probabilities for large transitions (areas iv and v) are slightly lower than for LHCSR1-V-7.5 (areas i and ii, Fig. 2g). The transitions in areas iv and v correspond to the transition between states II and III in

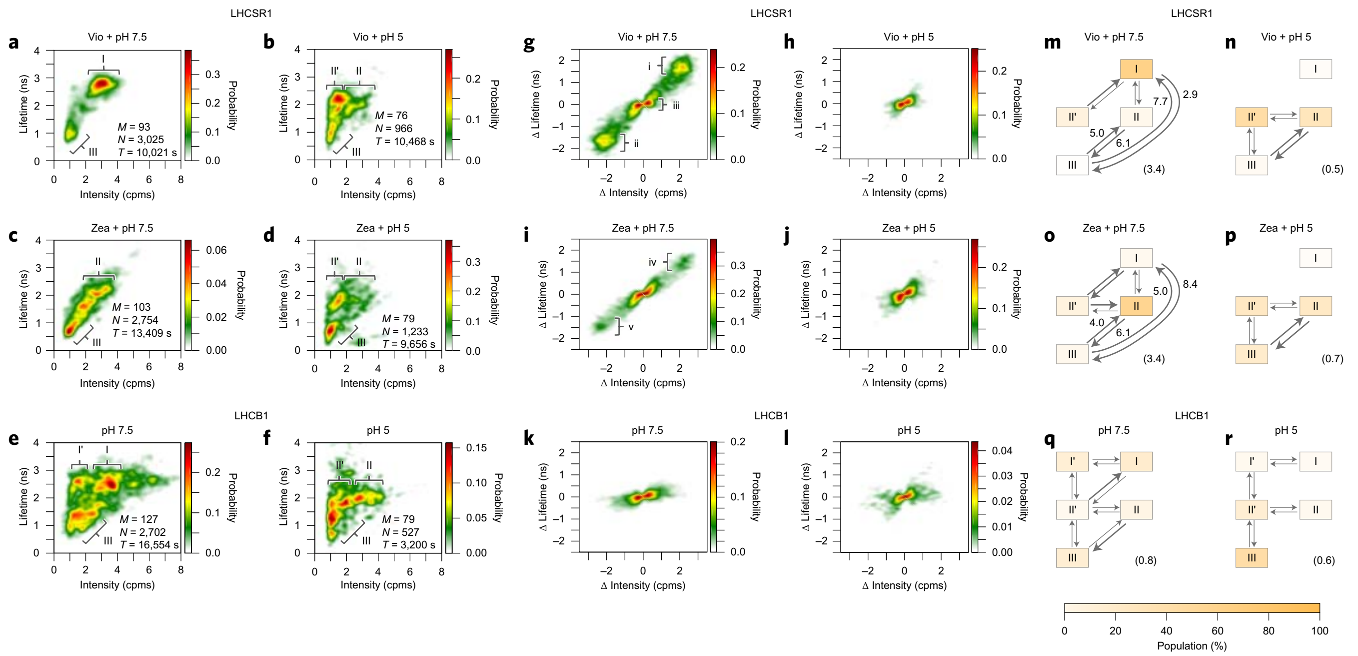

Figure 2 | Fluorescence intensity–lifetime probability distributions of single LHCSR1 and LHCB1 reveal protein dynamics. a–f, Fluorescence intensity–lifetime probability distribution of LHCSR1 with Vio at pH 7.5 (**a**) and pH 5 (**b**), Zea-enriched LHCSR1 at pH 7.5 (**c**) and pH 5 (**d**) and LHCB1 at pH 7.5 (**e**) and pH 5 (**f**). The two-dimensional histograms were constructed from all intensity–lifetime data sets consisting of each period exhibiting constant intensity. The total numbers of molecules (M) and data points (N) and the sum of dwell times of each period (T) used to make each histogram are shown in the lower right of each plot. The colour scale is normalized by the maximum probability in each plot. Four and five states were identified in the distribution of LHCSR1 and LHCB1, respectively, labelled I, I′, II, II′ and III (Supplementary Fig. 3). **g–l**, Fluorescence intensity–lifetime transition probability distributions for each sample. Transitions between levels of fluorescence intensity and lifetime (Δ Intensity and Δ Lifetime) were calculated by subtracting the values in a period before a transition from those after it. The colour scale is normalized to the maximum probability in each plot. Areas corresponding to representative transitions are labelled i–v. **m–r**, Schematics of protein dynamics in each sample. The thickness of each arrow is proportional to the rate of transition between the states. The transition rates (1/s) between states I and III and between II and III in LHCSR1-V-7.5 and LHCSR1-Z-7.5 are indicated next to each arrow. The average rate for each sample is shown in parentheses. Transitions with low probability (<1.5%) and within each state are not shown. The colour contrast of the box indicates the relative population, that is, the ratio of total dwell time, for each state. All rates and populations are listed in Supplementary Table 2. Q6

Fig. 2c, as shown in period 4 in Fig. 1c. The pH drop prevents large transitions in both LHCSR1 with Vio and Zea (Fig. 2h,j), showing that the protein dynamics are restricted at low pH. On the other hand, LHCB1 exhibits no large transitions at either pH (Fig. 2k,l).

Rates of conformational dynamics in single LHCSR1 and LHCB1. To better characterize these dynamics, the populations of each state and the rates of transitions between states were calculated, as shown in Fig. 2m–r and Supplementary Table 2. LHCSR1-V-7.5 (Fig. 2m) exhibits connectivity between the states, as indicated by arrows: fast dynamics between states II and III; biased dynamics between states I and III; strongly biased dynamics between states I and II′; and slow dynamics between states I and II. As a consequence, the relative population of the states was biased towards state I (active, or unquenched). Notably, the transition rate from state III to I is faster than that from state I to III. In contrast, as illustrated in Fig. 2o, for LHCSR1-Z-7.5, the transition rate from state I to state III is faster. The transition rate from state II to state III is also slightly faster. These changes in dynamics increase the bias in the population towards state III (quenched). Overall, similar to LHCSR1-V-7.5, LHCSR1-Z-7.5 exhibits connectivity between the states and rapid dynamics. This situation is quite different in LHCB1-7.5, where all states are connected by slow and almost equal dynamics and thus exhibit even populations (Fig. 2q).

Discussion

Microscopic mechanisms of protein dynamics. Here, we discuss the mechanisms behind the distinct functional conformations and functional dynamics of LHCSR1. The effect of xanthophyll composition acts predominantly on the dynamics of LHCSR1 at pH 7.5, where bias towards quenching is introduced by controlling the rates of conformational dynamics, as discussed above. The pH drop also biases the population towards the quenched states along this conformational coordinate (Supplementary Fig. 5). An illustration of the changing free-energy landscape is presented in Fig. 3b.

The three states (I, II and III) most probably lie along the same conformational coordinate, because of the direct proportionality between intensity and lifetime (Fig. 2a–f). Photophysically, this indicates a changing level of quenching of the emissive state. In the homologous LHCII, the emissive state has been shown to be localized on a trimer of chlorophyll[31,32]. Previous experiments on LHCII proposed that the carotenoid neighbouring the emissive chlorophyll trimer serves as a quencher for the excitation[19,26,28,29]. In LHCSR1, the carotenoid quenches the chlorophyll through the formation of a charge-transfer state between the chlorophyll and the carotenoid, and energy transfer to the carotenoid[25]. Thus, we propose that a conformational coordinate exists, as illustrated in Fig. 3a (Q_1), that controls the distance between the emissive chlorophyll and the carotenoid[33].

The pH drop causes two additional changes in the dynamics and relative populations of the states in LHCSR1 (Fig. 2n,p). First, the fast dynamics observed at pH 7.5 are reduced by an order of magnitude. Second, the populations of state I (active) and state II (partially quenched) move to state II′ (quenched). Thus, we speculate that the protonation event functions via rigidification of the structure, essentially locking the protein into a quenched conformation. These

NATURE CHEMISTRY DOI: 10.1038/NCHEM.2818

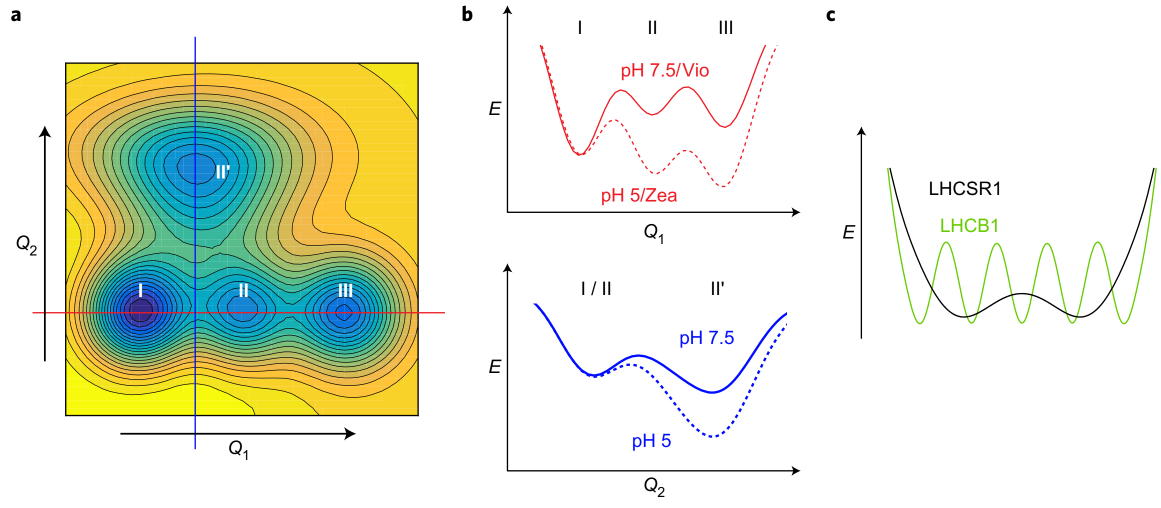

Figure 3 | Cartoon illustration of the free-energy landscape of LHCSR1. a, Contour map of the free-energy landscape of LHCSR1-V-7.5 plotted as a function of two generalized nuclear coordinates, Q_1 and Q_2. States I, II, III and II′ are defined in Fig. 2a–d (also Supplementary Fig. 3). **b**, Free-energy shifts triggered by changes in pH from 7.5 to 5 and xanthophyll composition from Vio to Zea, displayed for energy landscape slices along Q_1 (top) and Q_2 (bottom), indicated by red and blue lines, respectively, in **a**. The free energies of LHCSR1 at pH 7.5 with Vio (solid curves) and after xanthophyll conversion and/or pH drop (dotted curves) are shown. **c**, Free-energy landscape under low light conditions of LHCSR1 (black) compared to that of LHCB1 (green).

effects of pH drop are illustrated as a decrease in the free energy of the quenched state II′ (Fig. 3b, bottom). However, the conformational coordinate that connects these states (Fig. 3a, Q_2) has not yet been identified.

Regulated protein dynamics of LHCSR1. Based on the present results, we suggest a photoprotective cycle where the two regulatory parameters, pH and carotenoid composition, work in combination to protect the photosystem II reaction centre (PSII RC) against high light conditions by matching the arrival of excitation energy to the turnover rate of the RC. This is implemented by controlling the dynamics between the unquenched, or higher, fluorescence states (I and II) and the quenched, or lower, fluorescence states (II′ and III). The parameters give rise to a controller that operates as a closed-loop feedback system. Whereas proportional control regulates steady-state signals, here the combination of parameters creates an integral controller, which regulates intermittent signals[34,35]. The two regulatory parameters (pH and Zea) introduce two control elements that are designed to respond to the two types of intermittency in solar intensity: (1) step changes (clouds and shadows) are regulated by integral control and (2) ramp changes (sunrise, day-to-day weather variation and so on) are regulated by double integral control.

The feedback system functions by repetition of the following steps: (1) probing a pH change on the lumenal side (feedback signal); (2) adjusting the free-energy landscape in response to the pH change and sequential xanthophyll conversion (integral and double-integral control elements, respectively); (3) regulating the excitation energy input to the RC (manipulated variable), which (4) controls the electron transfer reactions in the RC (controlled object), which, in turn, drives lumenal pH.

Here, we describe a potential control scheme consistent with the results presented, using a framework in which a 'switch' moves between an active and a quenching terminal (Fig. 4) through the conformational dynamics of LHCSR1. Under low light conditions, corresponding to LHCSR1-V-7.5 (Fig. 4a), the rapid dynamics between active and quenching states provide a regulatory mechanism that serves as an on–off switch for the RC. At pH 7.5, the dynamics are biased towards the active state (state I), allowing excitation energy to efficiently reach the RC. When the light level increases (Fig. 4b), the pH on the lumenal side drops. This pH change lowers the potential levels of state II and II′ (Fig. 3b and Supplementary Fig. 5), and the rapid dynamics allow for a fast shift in population from state I (unquenched) to state II′ (quenched) via state II. Thus, the 'switch' is set to the quenching terminal via pH-integral control. If the light level decreases immediately, the pH increases and the bias returns to the active state (Fig. 4a). Conversely, when the light level remains high for a few minutes (Fig. 4c), Vio is enzymatically converted into Zea by the pH-activated enzyme VDE (violaxanthin de-epoxidase)[36] and binds to LHCSR1[11]. The Zea binding lowers the potential level of state III (quenched), making the quenching state dominant to adapt to the extended period of high light. Thus, the 'switch' remains set to the quenching terminal via pH-double-integral control (accumulation of protons leads to accumulation of the activated enzyme responsible for conversion of Vio to Zea). When the light level decreases and the lumenal pH increases (Fig. 4d), the potential levels of states II and II′ increase. Thus, the dynamics between state II and III—that is, switching between quenched and unquenched states—returns. However, the protein dynamics remain biased towards the quenched state, protecting against the rapid re-emergence of high light conditions. If the pH remains neutral (~1 h), then the Zea is converted into Vio, leading to a rise in the potential level of state II and the return of LHCSR1 to low light conditions (Fig. 4a).

Intrinsic protein dynamics of LHCSR1. In most organisms, relatively high light is required for LHCSR1 expression[7,8,14], suggesting a photoprotective role for LHCSR1, even in the absence of a pH drop. LHCSR1 at pH 7.5 remains in the quenching state for ~130 and ~250 ms, as estimated from transition rates from III to I and II in the presence of Vio and Zea, respectively (Supplementary Table 2). These times are sufficient for a doubly reduced and protonated plastoquinone (Q_B) in the PSII RC to be exchanged with an oxidized one in the quinone pool[37,38]. During this time, energy rapidly migrates throughout the LHC network, so even a single quenched LHCSR1 within this network can provide photoprotection. LHCSR1 was proposed to act on the LHCs associated not only with PSII[10] but also with the PSI complex[13]. These photoprotective timescales would also protect PSI, where the photoreaction is cycled on a similar millisecond time scale *in vivo*[39].

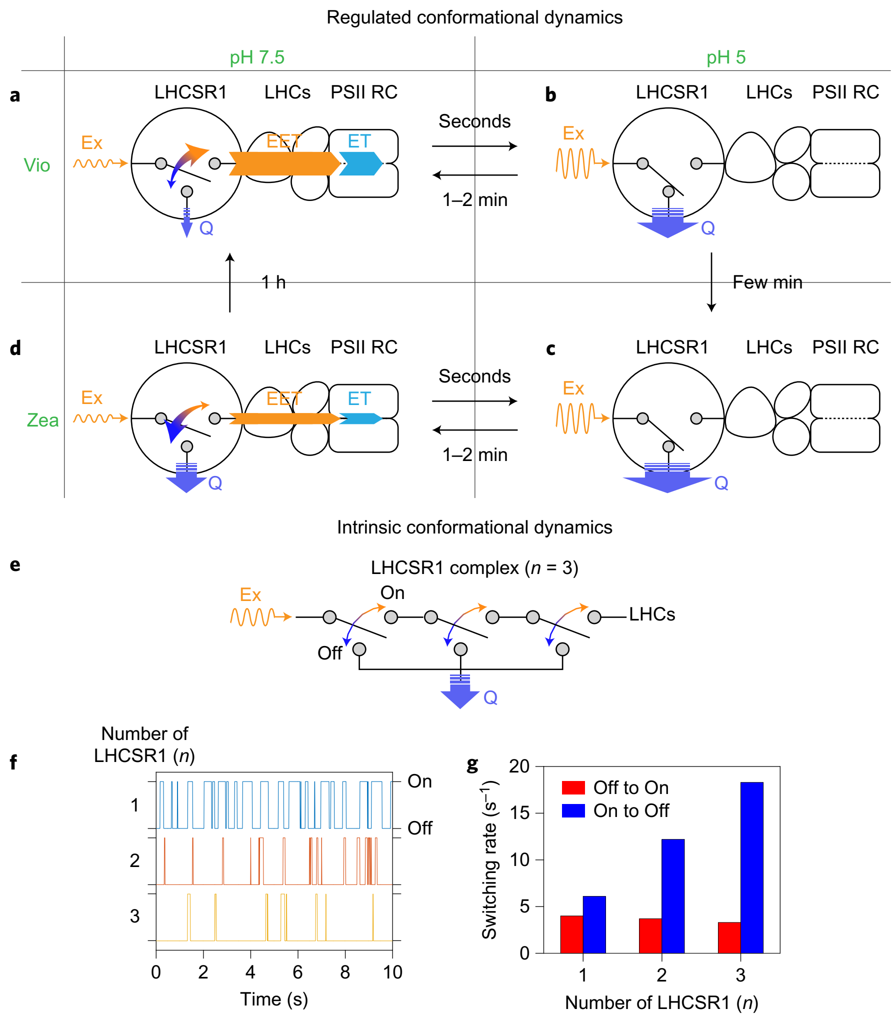

Figure 4 | Potential scheme of light-harvesting activity regulated through LHCSR1. a–d, Regulated conformational dynamics matching LHCSR1 function to different conditions: Vio/pH 7.5 (**a**), Vio/pH 5 (**b**), Zea/pH 5 (**c**) and Zea/pH 7.5 (**d**). Excitation (Ex) energy absorbed in LHCSR1 is transferred to one of two terminals: xanthophyll within LHCSR1, which can quench the energy (Q), or the LHC network via inter-complex excitation energy transfer (EET), through which the excitation reaches the RC, where charge separation and electron transfer (ET) occur. Switching between active and Q terminals (on and off states, respectively) is indicated by a two-headed arrow. **e–g**, Intrinsic conformational dynamics producing switching between active and Q, enhanced by incorporating multiple LHCSR1s in the antenna. The on–off switching behaviour was simulated (**f**) and its rate was estimated (**g**) as a function of the number of LHCSR1s (**e**). For more details, see Supplementary Fig. 9.

Although the average of number of LHCSR1s per RC is thought to be low (~0.5), the conformational dynamics ensure that even in the case of accumulation, the RC can be safely driven without decreasing its overall efficiency. We simulated the switching behaviour between on and off (active and quenched) states for the system as a function of number of LHCSR1s (Fig. 4e–g), where the off state comprises one or more LHCSR1s in the quenched state and the on state has no LHCSR1s in the quenched state (Supplementary Fig. 9). As the number of LHCSR1s increases, the on time when all LHCSR1s are in the active state decreases to reach a pulse-like instantaneous switching (Fig. 4f,g, blue bars), reducing the risk of producing reactive oxygen species[37]. Meanwhile, the off time when at least one LHCSR1 is in the quenched state does not strongly depend on the number of LHCSR1s (Fig. 4g, red bars) and remains comparable to the timescale of the RC reaction cycle. The accumulation of quenched complexes has been proposed to improve the photoprotective ability of PSII supercomplexes[40]. Currently, the number and position of LHCSR1 in the supercomplex as well as the photophysical dynamics and timescales of quenching remain ambiguous[25]. As this information becomes available, future research will allow the development of a detailed model of quenching in the photosystems as well as how quenching is controlled by the conformational states and dynamics characterized here.

Comparison between LHCs. LHCSR1 and LHCB1 are homologous, and their emissive properties span approximately the same range of intensity and lifetime, as illustrated in Fig. 2a,e, suggesting that they access a similar conformational space. However, the probability is more localized and the dynamics are much faster in LHCSR1 than in LHCB1 (Supplementary Table 2). The differences in populations and dynamics suggest free-energy landscapes of LHCSR1 and LHCB1 similar to those illustrated in Fig. 3c. LHCSR1 switches rapidly between states, while the states of LHCB1 are separated by potential barriers that are high enough to suppress the dynamics[41].

Previous experiments have characterized the major light-harvesting complex LHCII and the minor LHCs found in PSII at the single-molecule level under conditions that mimic high and low light[26,27,29]. First, similar to LHCSR1 and LHCB1, the population of LHCII shifts towards quenched states under conditions that mimic high light[26,29]. Previous experiments on LHCII observed an intensity histogram with a single peak that shifts downwards in intensity[26]. In contrast, the intensity histogram of LHCSR1 contains two peaks and the population shifts into the quenched emissive state (Supplementary Fig. 7). Notably, the minor LHCs do not exhibit a shift into quenched states[27]. In addition, an increase in the population of a fully quenched state (blinking) and a redshifted state were observed for LHCII, leading to the hypothesis that the protein conformational dynamics control switching between emissive states, as in the results presented here[26]. Second, the dynamics of LHCSR1 are faster than for other LHCs. The average rate of transitions between emissive states is ~0.1 s^{-1} for LHCII[29], and 0.8 s^{-1} for LHCB1 and 3.4 s^{-1} for LHCSR1. Overall, LHCSR1 thus exhibits more rapid dynamics than other LHCs, enabling faster re-equilibration[29].

Finally, an additional difference between LHCSR1 and LHCB1 emerges from further dividing the two-dimensional fluorescence intensity and lifetime histograms by survival time, as shown in Supplementary Fig. 6. This division reveals that the quenched conformations of LHCB1 exhibit enhanced photostability. It may be that the photostable conformations of a common ancestor of LHCB1 and LHCSR1 provided the evolutionary precursor for the photoprotection in LHCSR1.

We can speculate on the ecological niche in which LHCSR1 provides important photoprotective functionality. In the event of photodamage within the LHCs[42], the active complexes (state I) of LHCB1 are preferentially photodamaged (Supplementary Fig. 6c), increasing the relative population of quenched complexes to protect the PSII RC. In contrast, there is no preferential photodamage in LHCSR1 (Supplementary Fig. 6a,b). Thus, under extremely high light conditions, LHCSR1 may actually provide reduced photoprotection compared to LHCB1. Additionally, the timescales of the intrinsic conformational dynamics match the normal operation of the PSII RC. However, if the photosynthetic organism is exposed to environmental stress such as temperature and drought, the electron transfer chain may be compromised and no longer operate on these timescales[43]. The land area is associated with more stress, which may explain why LHCSR1 has been observed only in aqueous organisms and moss[44–46], which inhabits shady and wet environments and yet also exhibits alternative quenching mechanisms.

The observation of the conformational states and dynamics of LHCSR1 uncovers controlled protein dynamics that regulate photoprotective dissipation. The present work identifies two distinct states that most probably correspond to the distinct conformations responsible for photoprotective dissipation, which provide multi-timescale photoprotection against intermittency in solar intensity. Although photoprotection *in vivo* involves additional molecular machinery, such as interactions with other LHCs, the discovery of two distinct processes is a fundamental step towards understanding the feedback loop responsible for photoprotective dissipation. This understanding has the potential to identify key control points that may be useful for increasing yields in algal biofuels and crops and mimicking these processes in artificial solar energy devices.

Methods

The LHCSR1 complexes were isolated from transgenic tobacco plants expressing a 6His-tagged ppLHCSR1 sequence as previously reported[12]. The Vio-binding form was obtained from dark-adapted plants. For isolation of the Zea-binding form, thylakoids were incubated at pH 5 in the presence of 30 mM ascorbate for 2 h. The LHCB1 complexes were obtained by *in vitro* refolding of 6His-tagged LHCB1 as previously reported[47]. Pigment composition (Supplementary Table 1) was determined by HPLC analysis, as previously reported[48].

Stock solutions of 10 μM LHCSR1 and LHCB1 complexes were kept at −80 °C. The solutions were thawed immediately before experiments and diluted to 50–1,000 and 0.1–2 pM, respectively, with buffer containing 20 mM HEPES-KOH (pH 7.5) and 0.05 wt% *n*-dodecyl-α-D-maltoside and *n*-dodecyl-β-D-maltoside, respectively. For the low pH experiments, 40 mM MES-NaOH (pH 5) buffer, with the same detergent, was used. The enzymatic oxygen-scavenging systems were also added to the solution at final concentrations of 25 nM protocatechuate-3,4-dioxygenase and 2.5 mM protocatechuic acid and 50 nM pyranose oxidase, 100 nM catalase and 5 mM glucose for the pH 7.5 and 5 buffers, respectively, before dilution[49,50]. The sample cell consisted of a cavity built on top of a coverslip with a Viton spacer, sealed by another coverslip. The LHC complexes were attached to the surface by interactions between their His-tag and a Ni-NTA coating (MicroSurfaces).

Single-molecule measurements were carried out in a home-built confocal microscope. A Ti:sapphire laser (Vitara-S, Coherent; λ_c = 800 nm, $\Delta\lambda$ = 70 nm, 20 fs pulse duration, 80 MHz repetition rate) was focused into a nonlinear photonic crystal fibre (FemtoWhite 800, NKT Photonics) to generate a supercontinuum and then filtered (ET645/30×, Chroma) to produce excitation at ~640 nm (Supplementary Fig. 1). Excitation power was set to ~450 nJ cm^{-2} per pulse on the sample plane, producing ~4.8×10^4 excitations of single LHCSR1 per second. Sample excitation and fluorescence collection were performed by the same oil-immersion objective (UPLSAPO100XO, Olympus, NA 1.4). The fluorescence was passed through filters (FF02-685/40-25 and FF02-675/67-25, Semrock; ET700/75m, Chroma) and detected by an avalanche photodiode (SPCM-AQRH-15, Excelitas). Photon arrival time was recorded by a time-correlated single-photon counting module (PicoHarp 300, PicoQuant). The instrument response function for the apparatus was measured to be 0.35 ns (full-width at half-maximum). Fluorescence intensity and lifetime were analysed as described previously[29]. The probability distribution map (Fig. 2) was smoothed by two-dimensional Gaussian filtering. All periods observed in the time trace (Fig. 1) were classified into four and five states (I, (I′), II, II′ and III) based on the intensity–lifetime probability distribution of LHCSR1 and LHCB1, respectively (Supplementary Fig. 3). The relative populations were estimated by the percentage of total dwell time in each state, and the rates of transitions were found by an exponential fit of the different dwell time histograms (Supplementary Fig. 4).

Data availability. The data that support the plots within this Article and other findings are available from the corresponding author on request.

Received 9 December 2016; accepted 2 June 2017;
published online XX XX 2017

References

1. Amerongen, H. & Croce, R. Light harvesting in photosystem II. *Photosynth. Res.* **116,** 251–263 (2013).
2. Ruban, A. V., Johnson, M. P. & Duffy, C. D. The photoprotective molecular switch in the photosystem II antenna. *Biochim. Biophys. Acta* **1817,** 167–181 (2012).
3. Rochaix, J.-D. Regulation and dynamics of the light-harvesting system. *Annu. Rev. Plant Biol.* **65,** 287–309 (2014).
4. Erickson, E., Wakao, S. & Niyogi, K. K. Light stress and photoprotection in *Chlamydomonas reinhardtii*. *Plant J.* **82,** 449–465 (2015).
5. Berteotti, S., Ballottari, M. & Bassi, R. Increased biomass productivity in green algae by tuning non-photochemical quenching. *Sci. Rep.* **6,** 21339 (2016).
6. Kromdijk, J. *et al.* Improving photosynthesis and crop productivity by accelerating recovery from photoprotection. *Science* **354,** 857–861 (2016).
7. Peers, G. *et al.* An ancient light-harvesting protein is critical for the regulation of algal photosynthesis. *Nature* **462,** 518–521 (2009).
8. Bonente, G. *et al.* Analysis of lhcsr3, a protein essential for feedback de-excitation in the green alga *Chlamydomonas reinhardtii*. *PLoS Biol.* **9,** e1000577 (2010).
9. Alboresi, A., Gerotto, C., Giacometti, G. M., Bassi, R. & Morosinotto, T. *Physcomitrella patens* mutants affected on heat dissipation clarify the evolution of photoprotection mechanisms upon land colonization. *Proc. Natl Acad. Sci. USA* **107,** 11128–11133 (2010).
10. Tokutsu, R. & Minagawa, J. Energy-dissipative supercomplex of photosystem II associated with LHCSR3 in *Chlamydomonas reinhardtii*. *Proc. Natl Acad. Sci. USA* **110,** 10016–10021 (2013).
11. Pinnola, A. *et al.* Zeaxanthin binds to light-harvesting complex stress-related protein to enhance nonphotochemical quenching in *Physcomitrella patens*. *Plant Cell* **25,** 3519–3534 (2013).
12. Pinnola, A. *et al.* Heterologous expression of moss light-harvesting complex stress-related 1 (LHCSR1), the chlorophyll *a*-xanthophyll pigment–protein complex catalyzing non-photochemical quenching, in *Nicotiana* sp. *J. Biol. Chem.* **290,** 24340–24354 (2015).
13. Pinnola, A. *et al.* Light-harvesting complex stress-related proteins catalyze excess energy dissipation in both photosystems of *Physcomitrella patens*. *Plant Cell* **27,** 3213–3227 (2015).
14. Maruyama, S., Tokutsu, R. & Minagawa, J. Transcriptional regulation of the stress-responsive light harvesting complex genes in *Chlamydomonas reinhardtii*. *Plant Cell Physiol.* **55,** 1304–1310 (2014).
15. Liguori, N., Novoderezhkin, V., Roy, L. M., van Grondelle, R. & Croce, R. Excitation dynamics and structural implication of the stress-related complex LHCSR3 from the green alga *Chlamydomonas reinhardtii*. *Biochim. Biophys. Acta* **1857,** 1514–1523 (2016).
16. Liguori, N., Roy, L. M., Opacic, M., Durand, G. & Croce, R. Regulation of light harvesting in the green alga *Chlamydomonas reinhardtii* : the C-terminus of LHCSR is the knob of a dimmer switch. *J. Am. Chem. Soc* **135,** 18339–18342 (2013).

17. Ballottari, M. *et al.* Identification of pH-sensing sites in the light harvesting complex stress-related 3 protein essential for triggering non-photochemical quenching in *Chlamydomonas reinhardtii*. *J. Biol. Chem*. **291,** 7334–7346 (2016).
18. Dinc, E. *et al.* LHCSR1 induces a fast and reversible pH-dependent fluorescence quenching in LHCII in *Chlamydomonas reinhardtii* cells. *Proc. Natl Acad. Sci. USA* **113,** 7673–7678 (2016).
19. Ruban, A. V. *et al.* Identification of a mechanism of photoprotective energy dissipation in higher plants. *Nature* **450,** 575–578 (2007).
20. Staleva, H. *et al.* Mechanism of photoprotection in the cyanobacterial ancestor of plant antenna proteins. *Nat. Chem. Biol.* **11,** 287–291 (2015).
21. Bode, S. *et al.* On the regulation of photosynthesis by excitonic interactions between carotenoids and chlorophylls. *Proc. Natl Acad. Sci. USA* **106,** 12311–12316 (2009).
22. Holt, N. E. *et al.* Carotenoid cation formation and the regulation of photosynthetic light harvesting. *Science* **307,** 433–436 (2005).
23. Ahn, T. K. *et al.* Architecture of a charge-transfer state regulating light harvesting in a plant antenna protein. *Science* **320,** 794–797 (2008).
24. Wahadoszamen, M., Berera, R., Ara, A. M., Romero, E. & van Grondelle, R. Identification of two emitting sites in the dissipative state of the major light harvesting antenna. *Phys. Chem. Chem. Phys*. **14,** 759–766 (2012).
25. Pinnola, A. *et al.* Electron transfer between carotenoid and chlorophyll contributes to quenching in the LHCSR1 protein from *Physcomitrella patens*. *Biochim. Biophys. Acta* **1857,** 1870–1878 (2016).
26. Krüger, T. P. *et al.* Controlled disorder in plant lightharvesting complex II explains its photoprotective role. *Biophys. J.* **102,** 2669–2676 (2012).
27. Krüger, T. P. *et al.* The specificity of controlled protein disorder in the photoprotection of plants. *Biophys. J.* **105,** 1018–1026 (2013).
28. Krüger, T. P., Ilioaia, C., Johnson, M. P., Ruban, A. V. & van Grondelle, R. Disentangling the low-energy states of the major light-harvesting complex of plants and their role in photoprotection. *Biochim. Biophys. Acta* **1837,** 1027–1038 (2014).
29. Schlau-Cohen, G. S. *et al.* Single-molecule identification of quenched and unquenched states of lhcii. *J. Phys. Chem. Lett*. **6,** 860–867 (2015).
30. Natali, A. *et al.* Light-harvesting complexes (LHCS) cluster spontaneously in membrane environment leading to shortening of their excited state lifetimes. *J. Biol. Chem.* **291,** 16730–16739 (2016).
31. Novoderezhkin, V. I., Palacios, M. A., Van Amerongen, H. & Van Grondelle, R. Excitation dynamics in the LHCII complex of higher plants: modeling based on the 2.72 Å crystal structure. *J. Phys. Chem. B* **109,** 10493–10504 (2005).
32. Schlau-Cohen, G. S. *et al.* Pathways of energy flow in LHCII from two-dimensional electronic spectroscopy. *J. Phys. Chem. B* **113,** 15352–15363 (2009).
33. Wentworth, M., Ruban, A. V. & Horton, P. Thermodynamic investigation into the mechanism of the chlorophyll fluorescence quenching in isolated photosystem II lightharvesting complexes. *J. Biol. Chem*. **278,** 21845–21850 (2003).
34. Zaks, J., Amarnath, K., Kramer, D. M., Niyogi, K. K. & Fleming, G. R. A kinetic model of rapidly reversible nonphotochemical quenching. *Proc. Natl Acad. Sci. USA* **109,** 15757–15762 (2012).
35. Zaks, J., Amarnath, K., Sylak-Glassman, E. J. & Fleming, G. R. Models and measurements of energy-dependent quenching. *Photosynth. Res*. **116,** 389–409 (2013).
36. Arnoux, P., Morosinotto, T., Saga, G., Bassi, R. & Pignol, D. A structural basis for the pH-dependent xanthophylls cycle in *Arabidopsis thaliana*. *Plant Cell* **21,** 2036–2044 (2009).
37. Cardona, T., Sedoud, A., Cox, N. & Rutherford, A. W. Charge separation in photosystem II: a comparative and evolutionary overview. *Biochim. Biophys. Acta* **1817,** 26–43 (2012).
38. de Wijn, R. & van Gorkom, H. J. Kinetics of electron transfer from Q_A to Q_B in photosystem II. *Biochemistry* **40,** 11912–11922 (2001).
39. Hald, S., Nandha, B., Gallois, P. & Johnson, G. N. Feedback regulation of photosynthetic electron transport by NADP(H) redox poise. *Biochim. Biophys. Acta* **1777,** 433–440 (2008).
40. Chmeliov, J. *et al.* The nature of self-regulation in photosynthetic light-harvesting antenna. *Nat. Plants* **2,** 16045 (2016).
41. Van Oort, B., van Hoek, A., Ruban, A. V. & van Amerongen, H. Equilibrium between quenched and nonquenched conformations of the major plant light-harvesting complex studied with high-pressure time-resolved fluorescence. *J. Phys. Chem. B* **111,** 7631–7637 (2007).
42. Chan, T. *et al.* Quality control of photosystem II: lipid peroxidation accelerates photoinhibition under excessive illumination. *PLoS ONE* **7,** e52100 (2012).
43. Kalaji, H. M. *et al.* Chlorophyll *a* fluorescence as a tool to monitor physiological status of plants under abiotic stress conditions. *Acta Physiol. Plant*. **38,** 102 (2016). Q5
44. Alboresi, A., Caffarri, S., Nogue, F., Bassi, R. & Morosinotto, T. *In silico* and biochemical analysis of *Physcomitrella patens* photosynthetic antenna: identification of subunits which evolved upon land adaptation. *PLoS ONE* **3,** e2033 (2008).
45. Niyogi, K. K. & Truong, T. B. Evolution of flexible nonphotochemical quenching mechanisms that regulate light harvesting in oxygenic photosynthesis. *Curr. Opin. Plant Biol*. **16,** 307–314 (2013).
46. Morosinotto, T. & Bassi, R. in *Non-Photochemical Quenching and Energy Dissipation in Plants, Algae and Cyanobacteria* 315–331 (Springer, 2014).
47. Remelli, R., Varotto, C., Sandonà, D., Croce, R. & Bassi, R. Chlorophyll binding to monomeric light-harvesting complex; a mutation analysis of chromophore-binding residues. *J. Biol. Chem*. **274,** 33510–33521 (1999).
48. Croce, R., Weiss, S. & Bassi, R. Carotenoid-binding sites of the major light-harvesting complex II of higher plants. *J. Biol. Chem*. **274,** 29613–29623 (1999).
49. Aitken, C. E., Marshall, R. A. & Puglisi, J. D. An oxygen scavenging system for improvement of dye stability in single-molecule fluorescence experiments. *Biophys. J.* **94,** 1826–1835 (2008).
50. Swoboda, M. *et al.* Enzymatic oxygen scavenging for photostability without pH drop in single-molecule experiments. *ACS Nano* **6,** 6364–6369 (2012).

Acknowledgements

This work was supported as part of the Center for Excitonics, an Energy Frontier Research Center funded by the US Department of Energy, Office of Science, Office of Basic Energy Sciences under award no. DE-SC0001088 (MIT) and a CIFAR Azrieli Global Scholar Award to G.S.S.-C.

Author contributions

T.K., R.B. and G.S.S.-C. conceived and designed the experiments. T.K. and W.J.C. performed the experiments. T.K. and G.S.S.-C. analysed the data. A.P., L.D. and R.B. contributed materials and analysis tools. T.K. and G.S.S.-C. co-wrote the paper. All authors discussed the results and commented on the manuscript.

Additional information

Supplementary information is available in the online version of the paper. Reprints and permissions information is available online at www.nature.com/reprints. Publisher's note: Springer Nature remains neutral with regard to jurisdictional claims in published maps and institutional affiliations. Correspondence and requests for materials should be addressed to G.S.S.C.

Competing financial interests

The authors declare no competing financial interests.

NATURE CHEMISTRY DOI: 10.1038/NCHEM.2818

nchem.2818 Table of Contents summary

Photoprotection is crucial for the fitness of organisms that carry out oxygenic photosynthesis. LHCSR, a photosynthetic light-harvesting complex, has been implicated in photoprotection in green algae and moss. Now, single-molecule studies of LHCSR have revealed that multi-timescale protein dynamics underlie photoprotective dissipation of excess energy.

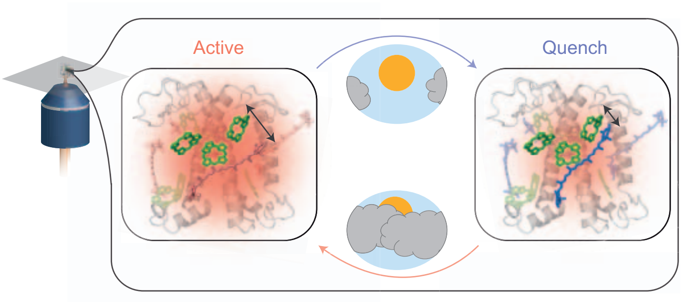

Journal: Nature Chemistry

Article ID: nchem.2818

Article title: Single-molecule spectroscopy of LHCSR1 protein dynamics identifies two distinct states responsible for multi-timescale photosynthetic photoprotection

Authors: Toru Kondo *et al*.

Q1	Author surnames have been highlighted - please check these carefully and indicate if any first names or surnames have been marked up incorrectly. Please note that this will affect indexing of your article, such as in PubMed.	
Q2	Please check that the expanded addresses are OK as presented.	
Q3	Please check that the sentence beginning "As shown in Fig. 1a" is OK as amended.	
Q4	Please define units cpms at first use.	
Q5	Ref 43 – please check inserted article number.	
Q6	Please check that the arrow thicknesses in Figure 2m–r are OK as presented.	